

Influence of Carbon Concentration on the Superconductivity in MgC_xNi_3

L. Shan¹, K. Xia², Z.Y. Liu¹, H.H. Wen¹, Z.A. Ren¹, G.C. Che¹, Z.X. Zhao¹

¹National Laboratory for Superconductivity, Institute of Physics,
Chinese Academy of Sciences, P.O. Box 603, Beijing 100080, China and

²International Center for Quantum Structures, Institute of Physics,
Chinese Academy of Sciences, P.O. Box 603, Beijing 100080, China

(Dated: November 12, 2018)

The influence of carbon concentration on the superconductivity (SC) in MgC_xNi_3 has been investigated by measuring the low temperature specific heat combined with first principles electronic structure calculation. It is found that the specific heat coefficient $\gamma_n = C_{en}/T$ of the superconducting sample ($x \approx 1$) in normal state is twice that of the non-superconducting one ($x \approx 0.85$). The comparison of measured γ_n and the calculated electronic density of states (DOS) shows that the effective mass renormalization changes remarkably as the carbon concentration changes. The large mass renormalization for the superconducting sample and the low T_c (7K) indicate that more than one kind of boson mediated electron-electron interactions exist in MgC_xNi_3 .

PACS numbers: 74.25.Bt, 74.20.Rp, 74.72.Jt

The recently discovered superconductor MgCNi_3 [1] with an anti-perovskite structure has attracted renewed attention, because it is a new intermetallic compound following the remarkable discovery of MgB_2 [2] and is thought to be very close to ferromagnetism (FM) due to a large proportion of Ni in each unit cell [3]. Experiments have shown that the superconductivity (SC) in MgC_xNi_3 is very sensitive to the content of carbon and disappears below about $x = 0.88$ [4]. Moreover, Ni-site doping with Cu (electron doping) and Co (hole doping) have very different effect[5].

Many efforts have been focused on the origin of SC in MgCNi_3 . Some researchers explored the possibility of conventional phonon-coupled pairing [6, 7]. However, various experiments and theoretical calculations have not given a consistent coupling constant λ in the frame of electron-phonon coupling (EPC) mechanism. For example, $\lambda \approx 1 - 1.6$ was estimated from the calculated plasma frequency (ω_p) and measured resistivity [8], while the measured upper critical field H_{c2} [9, 10, 11] suggested a much larger value of $\lambda \approx 2.5 - 3$. Furthermore, two discrepant values of $\lambda = 0.7$ [1] and 2.2 [10] were determined in the similar specific heat measurements by taking different approximations. Besides these confusing results, it has been proposed that EPC is possibly not the only contribution to the coupling mechanism in MgCNi_3 system [8, 10]. Opposed to the conventional pairing mechanism, it was suggested that FM and SC may coexist due to the ferromagnetic instability caused by the high density of electronic states (DOS) at the Fermi energy (E_F) [3, 12]. NMR experiment confirmed the presence of substantial ferromagnetic spin fluctuations in MgCNi_3 [13], while it also exhibited a clear coherence peak of the nuclear spin-lattice relaxation rate just below T_c , which is typical for an isotropic s-wave superconductor. More recently, Voelker *et al.* [14] proposed that MgCNi_3 could be a multiband superconductor with a conventional phonon mechanism [15] similar to MgB_2 [16]. Thus, the origin

of SC in MgCNi_3 is still controversial. One of the most illuminative methods is to study the influence of element-substitution on SC.

In this Letter, we compare the specific heat data of a superconducting MgC_xNi_3 with $x \approx 1$ and that of a non-superconducting one with $x \approx 0.85$. Using the tight-binding linear muffin-tin orbital (TB-LMTO) band method and coherent potential approximation (CPA) [17, 18], we investigate the carbon concentration dependence of the electronic structure of MgC_xNi_3 . Combining the results of the specific heat and band calculations, we propose a self-consistent picture to understand the reduced SC in non-stoichiometric MgC_xNi_3 .

Poly-crystalline samples of MgC_xNi_3 were prepared by powder metallurgy method. Details of the preparation were published previously [19]. The superconducting transition of the stoichiometric sample (SC1) with $T_c = 7K$ is shown in Fig. 1. A non-superconducting sample (NSC08) was synthesized by continually reducing the carbon component until the diamagnetism was completely suppressed. X-ray diffraction (XRD) patterns show nearly single phase in both samples. The lattice parameters a determined from XRD are 3.812\AA and 3.790\AA for SC1 and NSC08, respectively. By comparing these lattice parameters with the reported $a \sim x$ relation [4], we could estimate the carbon content as $x = 0.977$ and 0.850 for SC1 and NSC08, respectively. According to the $T_c \sim x$ relation presented in Ref [4], $x = 0.977$ corresponds to $T_c \approx 7K$ and $x = 0.850$ is very close to the critical stoichiometry of SC in MgC_xNi_3 , which is in good agreement with our experimental results. The temperature dependence of the normalized resistivity is shown in Fig. 1. The heat capacity data presented here were taken with the relaxation method [20] based on an Oxford cryogenic system Maglab, in which the heat capacity is determined by a direct measurement of the thermal time constant, $\tau = (C_s + C_{add})/\kappa_w$, here C_s and C_{add} are the heat capacity of the sample and addenda, respectively, while

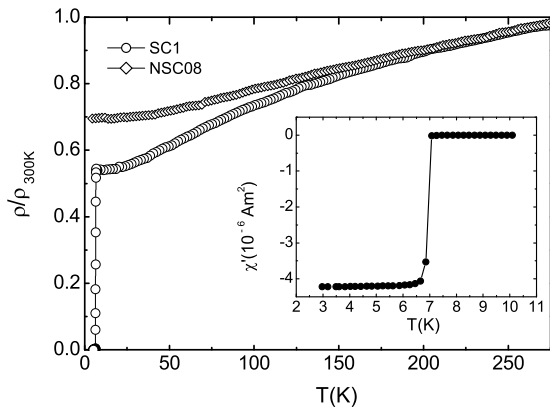


FIG. 1: The temperature-dependent resistivity (normalized by the value at 300K) of the samples SC1 and NSC08. Inset: The enlarged view of the superconducting transition in AC susceptibility measurement.

κ_w is the thermal conductance between the chip and a thermal link. During the measurement the sample was cooled to the lowest temperature under a magnetic field (field-cooling) followed by data acquisition in the warming up process. The addenda includes a small sapphire chip, a tiny Cernox temperature sensor, small amount of Wakefield thermal conducting grease and gold leads ($\phi 25\mu\text{m}$). All contributions to the heat capacity from the addenda have been measured separately and subtracted from the total specific heat before further analysis.

The typical low temperature specific heat at various magnetic fields up to 12 Tesla is presented in Fig. 2. For sample NSC08, all the data fall into an universal curve, indicating the independence of its specific heat on the magnetic field. For sample SC1, all the data above T_c are independent on the field, and the normal state extends to the whole temperature region investigated here when $H \geq 10T$. The upper critical field $H_{c2}(T)$ can be determined from the position of the specific-heat jump, and $H_{c2}(0) \approx 11T$ is then derived by extrapolating $H_{c2}(T)$ to 0K. In order to describe the specific heat data of NSC08 and the normal state data of SC1, we use the following expression:

$$C_n(T) = \gamma_n T + \beta T^3 + \delta T^5 \quad (1)$$

where the linear-T term is the electronic contribution with γ_n as Sommerfeld parameter, the second term represents the phonon contribution according to the Debye approximation, the last term is required to include deviations from the linear dispersion of the acoustic modes in extended temperature range. The fitting results are presented in Fig. 2, and the obtained parameters are shown in Table I. Besides the obvious difference between the Debye temperatures (Θ_D) of SC1 and NSC08 (due to the larger elastic modulus of NSC08 than that of SC1), a more prominent difference is found between the Som-

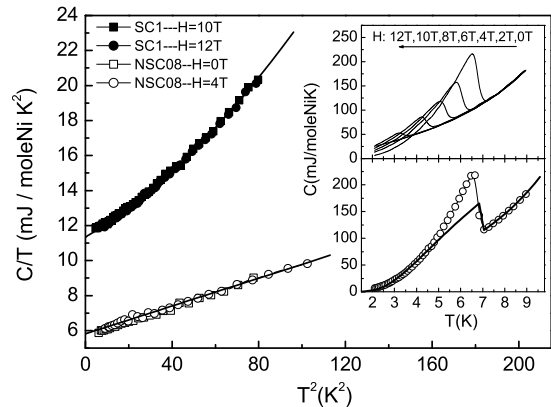


FIG. 2: A plot of C/T vs T^2 for MgCNi_3 (SC1) and $\text{MgC}_{0.85}\text{Ni}_3$ (NSC08) in various magnetic fields. The solid lines are fits to Eq. (1) as discussed in the text. The specific heat jump at the superconducting transition temperature is completely depressed by the field above 10T. Upper inset: The low-temperature specific heat for SC1 at various magnetic fields from 0T to 12T. Lower inset: Fitting for the zero-field specific heat data (open circles).

TABLE I: Fits to Eq. (1) for samples SC1 and NSC08.

sample	γ_n mJ/molNiK^2	β mJ/molNiK^4	δ mJ/molNiK^6	Θ_D K
SC1	11.3	0.075	0.00049	351
NSC08	5.8	0.040	0	434

merfeld parameters γ_n of these two samples, this is one of the main results in this work.

Before further analysis, we at first investigate the specific heat data of the superconducting sample SC1 in zero field, as shown in the lower inset of Fig. 2. The solid curve represents the theoretical fits, the part above T_c is the fitting result to the normal state data of SC1 as mentioned above, while the part below T_c is an attempt to describe the data using the specific heat expression of conventional superconductor: $C_{es} = A \exp(-\Delta(0)/k_B T)/T^{1.5}$, in which A is a function of zero-temperature energy gap $\Delta(0)$ and the normal-state DOS $g(0)$. This equation is a low temperature approximation and is not adequate above $0.8T_c$ where $\Delta(T)$ has substantially deviated from $\Delta(0)$. This conventional expression can fit our data below $0.8T_c \approx 5K$ quite well, though the returned $\Delta(0)$ (1.46meV) leads to a large value of $2\Delta(0)/k_B T_c \approx 5$ comparing with the weak coupling value 3.5. This indicates that MgCNi_3 is a strong coupling superconductor, being consistent with the large value of $\Delta C/\gamma_n T_c \approx 1.7$ (the expected value for weak coupling is 1.43), where ΔC is the specific heat jump at T_c .

As shown above, the specific heat coefficient γ_n of SC1 is almost twice that of NSC08. In the frame of strong coupling mechanism, given the value of γ_n and $N(E_F)$,

an effective mass renormalization factor (λ) can be estimated from the following relation [21, 22]

$$\gamma_n = \frac{\pi^2}{3} k_B^2 (1 + \lambda) N(E_F) \quad (2)$$

In order to obtain $N(E_F)$, we have calculated the electronic structures using a TB-LMTO method based on Green function formalism [17] within the atomic sphere approximation (ASA). The parameterized exchange-correlation potential of Ref [24] and the scalar-relativistic Dirac equation [23] were employed. The coherent potential approximation (CPA) used in our calculation allowed us to study the electronic structure of MgC_xNi_3 for any Carbon concentration. In the crystal structure of cubic antiperovskite-type MgCN_3 , the atoms occupy the positions Mg (0,0,0), C (0.5,0.5,0.5), and Ni (0.5,0.5,0), (0.5,0,0.5), (0,0.5,0.5). Self-consistency was reached using 1000 k-points within the irreducible wedge of the simple cubic Brillouin zone. In the calculations, we adopted the experimentally determined [4] relation between the lattice parameter a and the carbon concentration x . A fixed radii proportion as 2.078 : 1 : 1.617 (Mg:C:Ni) was taken for the stoichiometric situation ($x = 1$), and only the radii of carbon-site was reduced with decreasing x .

The DOS of MgC_xNi_3 for $x = 1$ are presented in the upper inset of Fig. 3, which is consistent with the reports of other groups [6, 8, 25, 26]. The π^* antibonding states of Ni-3d and C-2p are located just below E_F , yielding a high DOS peak whose height is proved to be sensitive to the exact method. Fortunately, the obtained value of $N(E_F) = 4.53 \text{ eV}^{-1}\text{cell}^{-1}$ is not far away from the result of general potential linearized augmented plane wave method ($4.99 \text{ eV}^{-1}\text{cell}^{-1}$) [8] and that of full-potential LMTO method ($4.57 \text{ eV}^{-1}\text{cell}^{-1}$) [12], which is a good starting point for the following consideration of the doping effect.

Fig. 3 shows the evolution of the DOS around Fermi level with the change of carbon concentration x in MgC_xNi_3 . It is found that the Fermi level slightly shifts towards low energy with the decreasing x , while the Ni3d-C2p antibonding peak is depressed remarkably. In the nearest-neighbor approximation, the degeneration of this DOS peak indicate that the carbon-site vacancies locally break the hybridization between Ni-3d and C-2p orbitals and hence lead to a redistribution of the electronic states. Atom-resolved DOS shows that the near- E_F DOS peak of Ni-3d component and that of C-2p component do not depart from each other with decreasing x , indicating that carbon-site vacancies does not destroy the Ni3d-C2p bond for all carbon concentrations investigated here. Therefore, the decrease of the peak possibly means the enhanced itinerancy of electrons. As shown in Fig. 3, the depressed DOS peak just below E_F results in a notable reduction of $N(E_F)$. The dependence of $N(E_F)$ on the carbon concentration is presented in Fig. 4. We can see a obvious decrease of $N(E_F)$ from 4.26eV^{-1} at $x = 0.977$

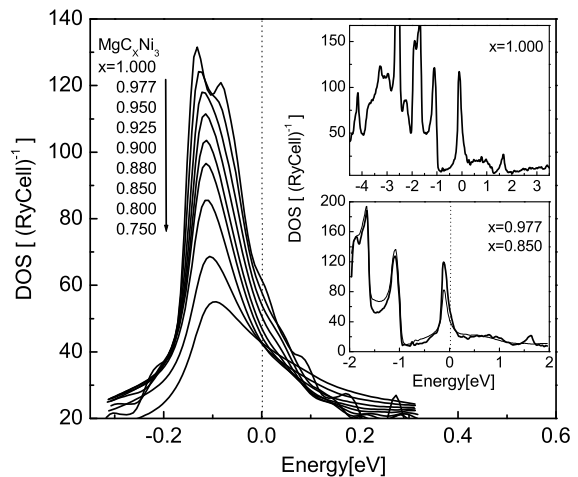


FIG. 3: Electronic DOS of MgC_xNi_3 for various carbon concentration calculated within the ASA. The dotted line indicate the Fermi level. Upper inset: Electronic DOS of MgCNi_3 in a larger energy scale. Lower inset: Redistribution of DOS with the change of carbon concentration. The thick solid line and thin one corresponds to $x = 0.977$ and 0.85 , respectively.

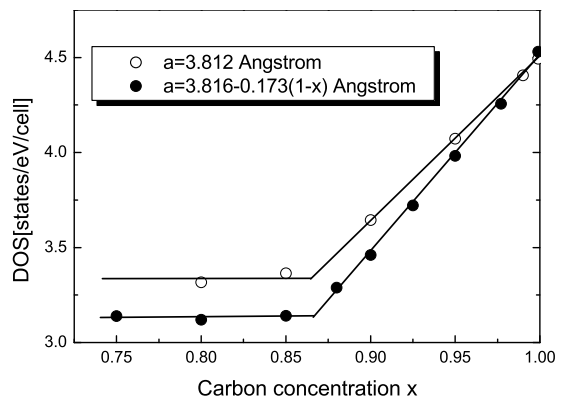


FIG. 4: The dependence of $N(E_F)$ of MgC_xNi_3 on carbon concentration. $N(E_F)$ for fixed $a = 3.812\text{\AA}$ is also calculated as a comparison. The solid lines are guides to eyes.

to 3.14eV^{-1} at $x = 0.85$. Moreover, the doping dependence of $N(E_F)$ is linear above a critical doping $x_c \approx 0.88$ which is very close to the carbon content in NSC08 and also the lower limit of the carbon concentration for SC in MgC_xNi_3 [4]. Below x_c , the doping dependence of $N(E_F)$ becomes much weaker than that above x_c .

By inserting the experimental value of γ_n and the calculated $N(E_F)$ into Eq(2), we can determine the coupling constant as $\lambda = 2.37$ and 1.35 for the samples SC1 and NSC08, respectively. The former is close to that reported by Wälte *et al.* [10], while the remarkable difference in the coupling strength between a superconducting sample and a carbon-deficient non-superconducting one is for the first time found in the MgC_xNi_3 system. However, applying $\lambda = 2.37$ to the McMillan's T_c formula [27]

$T_c = \frac{\Theta_D}{1.45} e^{-\frac{1+\lambda}{\lambda}}$ gives rise to $T_c > 30K$, which seems to be too large as compared to experimental value $T_c = 7K$. In other words, $T_c = 7K$ corresponds to $\lambda = 0.42$, which is much smaller than the value determined here. This contradiction can be resolved if we adopt the picture that there are two kinds of boson-mediated electron-electron interactions, for example, electron-phonon coupling (EPC) and spin fluctuation (SF) [8, 10]. Due to the different effect of the spin fluctuations on mass renormalization and superconducting properties, it should add in the mass renormalization term and subtract in the pairing term for SC. So in the frame of strong coupling, the specific heat determined λ has two contributions: $\lambda = \lambda_{ph} + \lambda_{spin}$. Similarly, the simplified McMillan's T_c formula should be modified as [8]

$$T_c = \frac{\Theta_D}{1.45} e^{-\frac{1+\lambda_{ph}+\lambda_{spin}}{\lambda_{ph}-\lambda_{spin}}} \quad (3)$$

Using the determined parameters for sample SC1 (namely, $\lambda = 2.2$, $T_c = 7K$ and $\Theta = 351K$), one obtains $\lambda_{ph} - \lambda_{spin} = 0.95$ from Eq.(3). Combining this result with $\lambda_{ph} + \lambda_{spin} = 2.37$, we determine the strength of both EPC and electron-paramagnon coupling as $\lambda_{ph} = 1.66$ and $\lambda_{spin} = 0.71$. Firstly, by assuming that λ_{spin} is invariable with the decreasing carbon concentration, we could obtain $\lambda_{ph} = 0.64$ for sample NSC08. This suggests a strong dependence of the EPC strength on the carbon concentration in MgC_xNi_3 . For NSC08, $\lambda_{ph} = 0.64$ has become smaller than $\lambda_{spin} = 0.71$, which is closely associated with the disappearance of SC. Secondly, on the assumption that $x = 0.85$ is the critical stoichiometry for SC, i.e., $\lambda_{ph} = \lambda_{spin}$, we obtain $\lambda_{ph} = \lambda_{spin} = 0.665$. This indicates a 6% decrease of λ_{spin} from $x = 0.977$ to $x = 0.85$. However, λ_{ph} is lost near 60% in the same system, which seems to be responsible for the suppression of SC in MgC_xNi_3 .

We have been aware of some recent calculations [12, 26] suggesting that both Co doping and Cu doping in $MgCNi_3$ lead to a reduction of $N(E_F)$, which seems to be critical in depressing SC in this system ($MgCNi_{3-x}Y_x$ [Y=Co or Cu]). However, these investigations were based on the ordered substitutions, i.e., $x=1, 2$ or 3 , which is somewhat away from the key problem because the solubility of Cu is limited to 3% ($x = 0.1$) in technology and the bulk SC disappears for only 1% Co doping ($x = 0.03$). Our further calculations did not show obvious reduction of $N(E_F)$ in this doping range. Therefore, some necessary investigations on the variation of the EPC in this system must be supplemented.

In summary, we have investigated the specific heat data in MgC_xNi_3 system and found a remarkable difference between the Sommerfeld parameters of a superconducting sample ($x \approx 1$) and a non-superconducting one ($x \approx 0.85$). Band calculations reveal a distinct decrease of the density of the electronic states at Fermi

level with the decreasing carbon concentration. Further analysis indicate that there is more than one kind of boson-mediated electron-electron interactions existing in MgC_xNi_3 system. In the frame of strong coupling theory, a substantial depression of the electron-phonon coupling caused by the decrease of carbon concentration is for the first time found in this system and seems to be responsible for the impairment of its superconductivity.

This work is supported by the National Science Foundation of China (NSFC 19825111, 10074078), the Ministry of Science and Technology of China (project: nkbrsf-g1999064602), and Chinese Academy of Sciences with the Knowledge Innovation Project.

-
- [1] T. He *et al.*, Nature (London) **411**, 54 (2001).
 - [2] J. Nagamatsu *et al.*, Nature (London) **410**, 63 (2001).
 - [3] H. Rosner *et al.*, Phys. Rev. Lett. **88**, 027001 (2002).
 - [4] T. G. Amos *et al.*, Solid State Communication **121**, 73 (2002).
 - [5] M. A. Hayward *et al.*, Solid State Communication **119**,491 (2001).
 - [6] J. H. Shim, S. K. Kwon, and B. I. Min, Phys. Rev. B **64**, 180510 (2001).
 - [7] S. B. Dugdale and T. Jarlborg, Phys. Rev. B **64**, 100508 (2001).
 - [8] D. J. Singh and I. I. Mazin, Phys. Rev. B **64**, 140507 (2001).
 - [9] S. Y. Li *et al.*, Phys. Rev. B **64**, 132505 (2001).
 - [10] A. Wälte *et al.*, cond-mat/0208364.
 - [11] Z. Q. Mao *et al.*, cond-mat/0105280.
 - [12] I. R. Shein, N. I. Medvedeva and A. L. Ivanovskii, cond-mat/0107010.
 - [13] P. M. Singer *et al.*, Phy. Rev. Lett. **87**, 257601 (2001).
 - [14] K. Voelker and M. Sigrist, cond-mat/0208367.
 - [15] D. F. Anterberg *et al.*, Europhys. Lett. **48**, 449 (1999) and Phys. Rev. B **60**, 14868 (1999).
 - [16] H. J. Choi *et al.*, Nature **418**, 758 (2002).
 - [17] I. Turek *et al.*, *Electronic Structure of Disordered Alloys, Surfaces and Interfaces* (Kluwer, Boston-London-Dordrecht, 1997).
 - [18] O.K. Andersen, O. Jepsen, and D. Glötzel, in *Highlights in Condensed Matter Theory*, edited by F. Bassani, F. Fumi and M. P. Tosi (North-Holland, Amsterdam, 1985), p. 59.
 - [19] Z. A. Ren *et al.*, Physica C **371**, 1 (2002).
 - [20] R. Bachmann *et al.*, Rev. Sci. Instrum. **43**, 205 (1972).
 - [21] A. Migdal, Sov. Phys. JETP **7**, 916 (1958).
 - [22] G. Rickayzen, *Green's Functions and Condensed Matter*, edited by N. H. March and H. N. Dalglish, (1980) Chap.7.
 - [23] D. D. Koelling and B. N. Harmon, J. Phys. C: Solid State Phys. **10**, 3107 (1977).
 - [24] S. H. Vosko, L. Wilk, and M. Nusair, Can. J. Phys. **58**, 1200 (1980).
 - [25] In Gee Kim, Jae Il Lee and A. J. Freeman, Phys. Rev. B **65**, 064525 (2002).
 - [26] I. R. Shein *et al.*, Phys. Rev. B **66**, 024520 (2002).
 - [27] W. L. McMillan, Phy. Rev. **167**, 331 (1968).